Abstract of a paper submitted for presentation at the Third Annual Inverse Problems in Engineering Seminar, Mechanical Engineering Dept., Michigan State University, East Lansing, MI 48824, June 25-26, 1990.

SHAPE DETERMINATION VIA OPTIMIZATION IN MULTIPLY CONNECTED DOMAINS

George S. Dulikravich
Penn State University, Dept. of Aero. Eng.
University Park, PA 16802, USA

During the past seven years a new method has been developed [1] and is been constantly improved, that allows a thermal cooling system designer to determine proper sizes, shapes, and locations of coolant passages (holes) in, say, an internally cooled turbine blade. Using our method this can be achieved by simultaneously enforcing temperature and heat flux distribution on , say, the hot outer surface of the blade , and separate temperature distributions on the surfaces of each of the holes. This is an overspecified problem which is solved by allowing the sizes, locations, and shapes of the holes to adjust iteratively until the final multiply connected configuration satisfies all overspecified boundary conditions and the governing Laplace's equation for the temperature field. The problem is solved by minimizing an error function expressing the difference between the specified and the computed hot surface heat flux. Whenever an optimization algorithm is used, there is always a problem of terminating the process by inadvertently finding a local minima. In addition, there is a problem of underiteration or insufficient accuracy which has been recognized in the field of numerical inverse methodologies.

To illustrate this problem, we have considered a test case consisting of a disk shaped domain with a thick coating of another material. The disk had a large centrally located hole (Fig. 1). There is a known analytical solution for a steady state temperature field in such doubly-connected composite circular domain when constant temperatures are specified on the outer boundary and the inner (hole) boundary. We have decided to use the corresponding analytical constant heat flux on the outer surface and the original temperature distributions, and try to satisfy these overspecified thermal boundary conditions by drilling three holes (Fig. 1) instead of one hole. Using our methodology, sizes of two holes have been reduced to practically zero (Fig. 1), while the third hole enlarged and became practically indistinguishable from the correct one-hole configuration. The convergence history of the optimization process (Fig. 2) indicates that the total count of thermal field analysis calls was 636 in order to reduce the L-2 norm of the surface integrated error to 0.1%. Obviously, the thermal field analysis routine should be as efficient as possible. For this reason we have used our version of a Boundary Element Method (BEM). Notice (Fig.3) that if we would have terminated the iterative process when the error was seemingly acceptably low (1.868%), the sizes and locations of the holes would have been unacceptably incorrect. In conclusion, a highly efficient analysis algorithm should be used until a convergence level of less than 0.1% error is achieved.

In the case of three holes where their initial sizes were identical and they were initially located at the same radial distance and spaced 120 degrees apart (Fig.4), each of the three holes changed its size and location equally since there was no preference for treating any of the holes differently. The apparently low error of the final converged solution (Fig. 5) was possible for two reasons. The thermal conductivities of the disk and the outer ring coating were considerably different. Also, we did not minimize local L-2 norm of the error at each point on the outer surface. Instead, we have minimized a circumferentially integrated error, which allows for a significant oscillation of the final outer surface flux.

In the case of four holes (Fig. 6), we attempted to satisfy constant temperature and constant heat flux on the outer surface of the coating by initially creating a doubly-symmetric configuration, that is each hole had identical diameter and symmetrical spacing with respect to the origin. The final result (Fig. 6) indicates that two holes slightly shrunk, while the other two holes enlarged. At the same time, all four holes drifted towards the origin. Recall that the correct solution involves only one large hole that is centrally located. Consequently, the convergence history (Fig. 7) indicates that it is practically impossible to reduce the error for this four-hole configuration below approximately 2.8%. The configuration evolution process is depicted in Fig. 8, while Fig. 9 shows the initial (dashed line) and the converged (full line) surface heat flux distribution. The analytically correct solution corresponding to one large hole has constant surface heat flux. The CPU time requirement evolution is depicted in Fig. 10. Despite the symmetry of the initial multiply-connected configuration, the surface discretization, and the thermal boundary conditions, an apparent diagonal asymmetry has developed. In other words, one pair of holes was apparently treated somewhat differently from the second pair of holes. We suspected that one-sided differencing used in the evaluation of gradient in the optimization algorithm was the reason for this phenomena. When recoding the optimization algorithm so that it used central differencing instead, identical results were obtained except that the total CPU time increased by about 60%. In conclusion, any new software for multiply-connected configurations should be first tested on multi-symmetric problems where they should maintain the multi-symmetry. Only then can such software be applied with full confidence to the inverse shape design in arbitrary multiply-connected configurations.

[1] Dulikravich, G.S.,"Inverse design and active control concepts in strong unsteady heat conduction", Appl. Mechanics Rev., Vol.41,No.6,June 1988, pp.270-277.

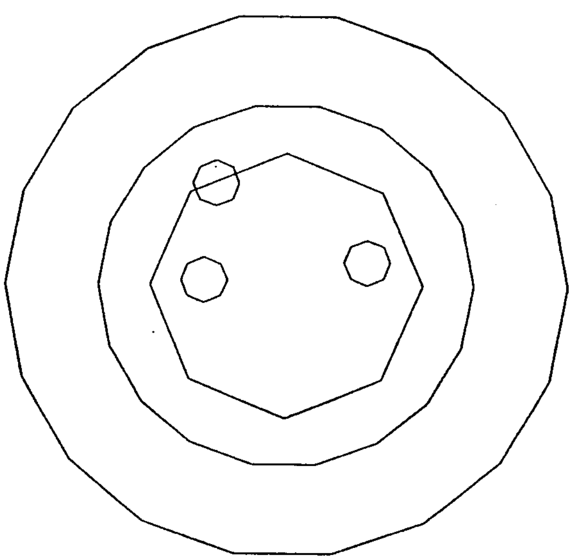

Fig. 1

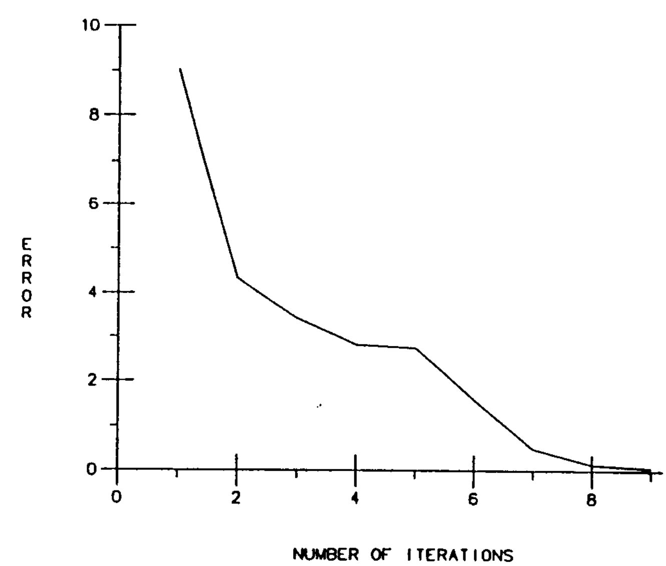

Fig. 2

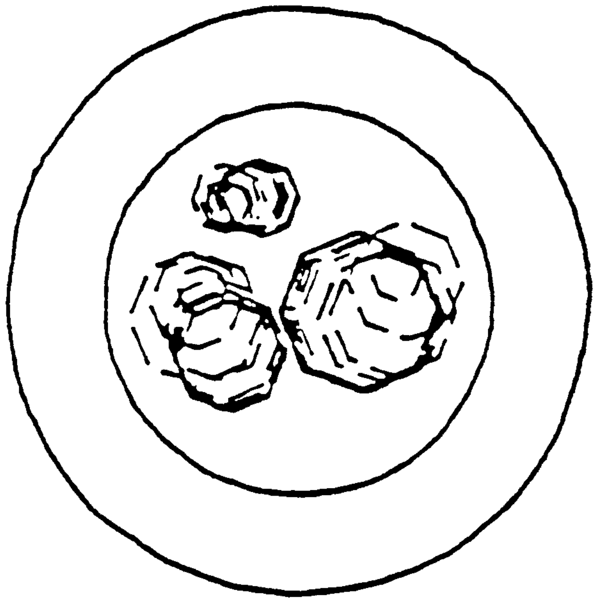
Fig. 3

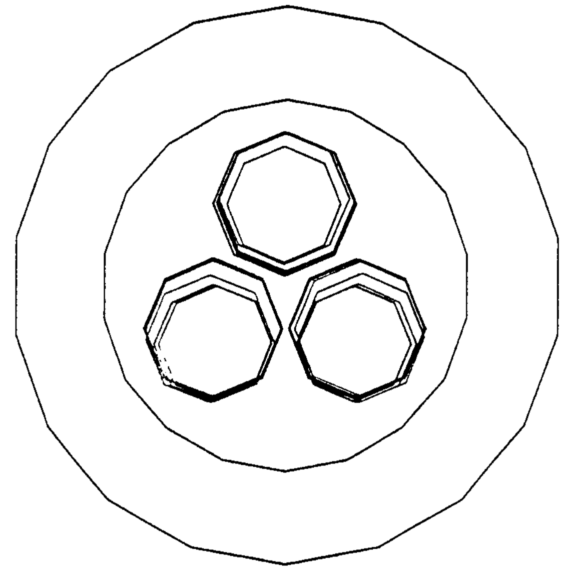
Fig. 4

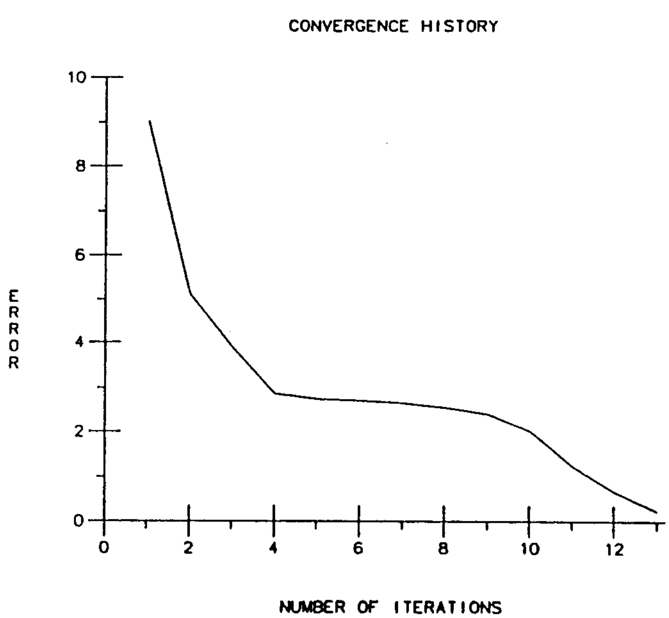

Fig. 5

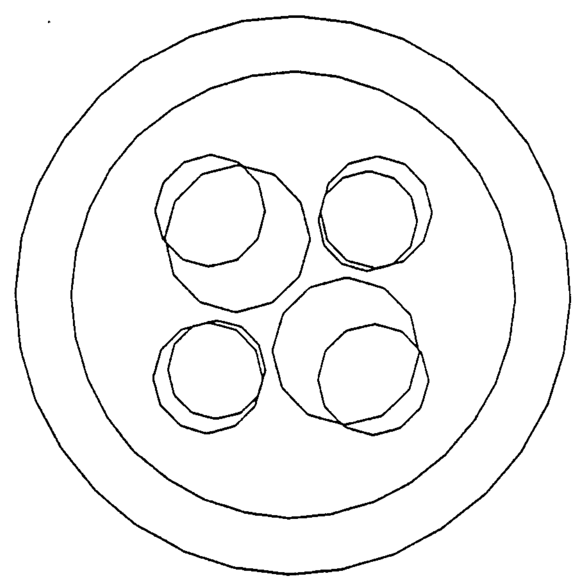
Fig. 6

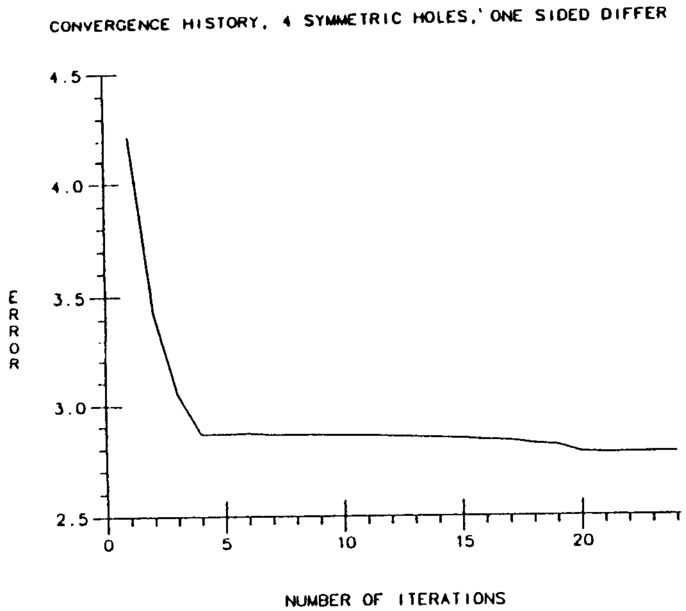

Fig. 7

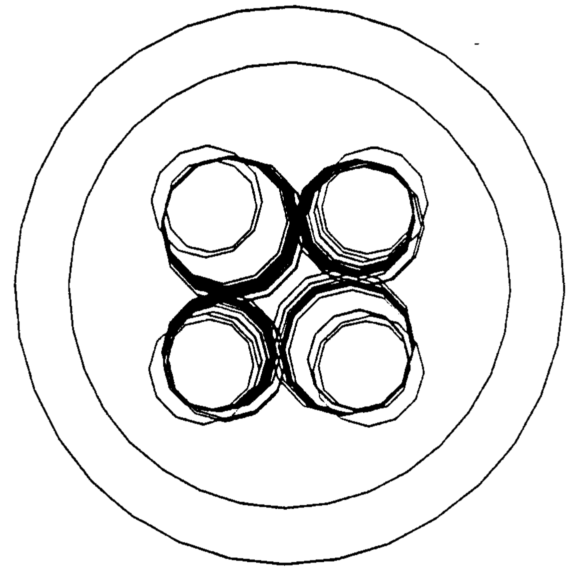

Fig. 8

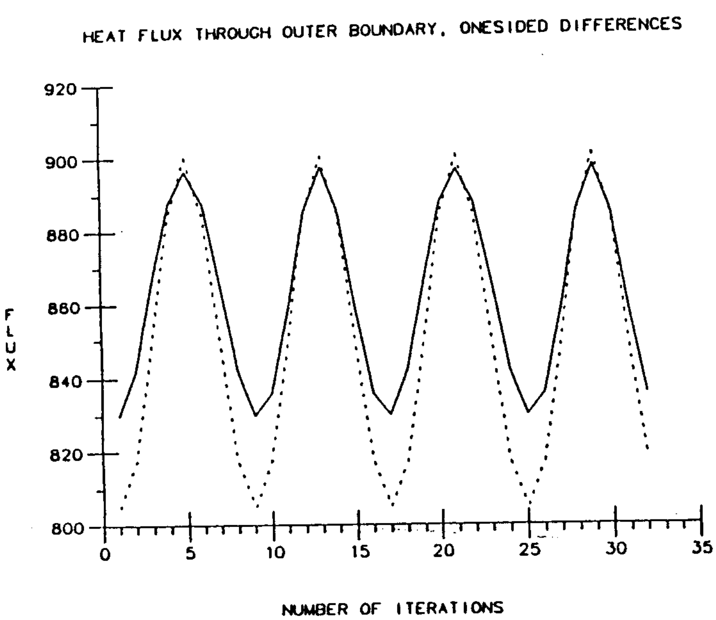

Fig. 9

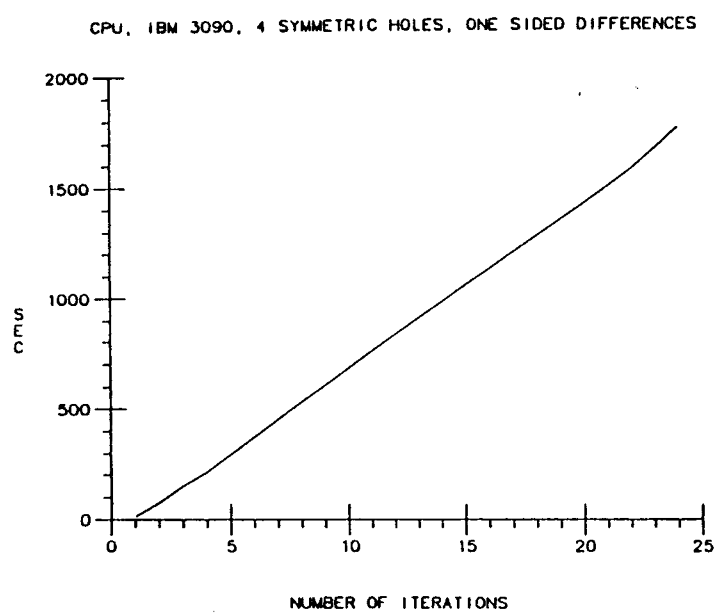

Fig. 10